Available online at www.sciencedirect.com
ScienceDirect
Biochimica et Biophysica Acta 1768 (2007) 1541–1549
Biochimica et Biophysica Acta BBA
www.elsevier.com/locate/bbamem

Electron spin-echo studies of spin-labelled lipid membranes and free fatty acids interacting with human serum albumin

Francesco De Simone [a], Rita Guzzi [a], Luigi Sportelli [a], Derek Marsh [b], Rosa Bartucci [a,*]

[a] *Dipartimento di Fisica, Laboratorio di Biofisica Molecolare and UdR CNISM, Università della Calabria, I-87036 Arcavacata di Rende (CS), Italy*
[b] *Max-Planck-Institut für biophysikalische Chemie, Abteilung Spektroskopie, D-37077 Göttingen, Germany*

Received 28 November 2006; received in revised form 29 January 2007; accepted 12 February 2007
Available online 3 March 2007

Abstract

Human serum albumin (HSA) is an abundant plasma protein that transports fatty acids and also binds a wide variety of hydrophobic pharmacores. Echo-detected (ED) EPR spectra and D_2O-electron spin echo envelope modulation (ESEEM) Fourier-transform spectra of spin-labelled free fatty acids and phospholipids were used jointly to investigate the binding of stearic acid to HSA and the adsorption of the protein on dipalmitoyl phosphatidylcholine (DPPC) membranes. In membranes, torsional librations are detected in the ED-spectra, the intensity of which depends on chain position at low temperature. Water penetration into the membrane is seen in the D_2O-ESEEM spectra, the intensity of which decreases greatly at the middle of the membrane. Both the chain librational motion and the water penetration are only little affected by adsorption of serum albumin at the DPPC membrane surface. In contrast, both the librational motion and the accessibility of the chains to water are very different in the hydrophobic fatty acid binding sites of HSA from those in membranes. Indeed, the librational motion of bound fatty acids is suppressed at low temperature, and is similar for the different chain positions, at all temperatures. Correspondingly, all segments of the bound chains are accessible to water, to rather similar extents.

Keywords: Electron spin resonance; Electron spin echo envelope modulation (ESEEM); Echo-detected spectra; Water accessibility; Librational motion

1. Introduction

Human serum albumin (HSA) is the most abundant plasma protein of the circulatory system. It contributes significantly to the blood osmotic pressure and to transport and regulatory processes [1]. Combining diverse affinities and wide specificity, it binds a variety of biological compounds such as metals, metabolic amino acids, hormones, anaesthetics, hydrophobic and amphipathic molecules [1–3]. HSA binds common drugs such as diazepam, warfarin and ibuprofen, and, in particular, shows a strong affinity to bind reversibly and non-covalently fatty acids for which it is the major transport protein to cell compartments [1]. By this molecular mechanism, the concentration of free fatty acids in the circulation is limited and the supply to mammalian cells ensured. Several studies have focused on the nature and location of the fatty acid binding sites in serum albumin [4–14]. It is found that there are several sites for unesterified fatty acids, which are located in different domains of the protein, and possess different orientations and amino acid environments [10,11]. The binding affinity depends on the length of the fatty acid chain: it increases with increasing chain length between 8 (octanoic) and 18 (stearic) carbon atoms, and then decreases for very long-chain fatty acids (alkyl chain >18 carbons) [11,13]. For the same ligands, there are multiple binding sites, which may be occupied simultaneously [4,6]. In the various binding sites, the alkyl chains of the fatty acids are accommodated in long and narrow hydrophobic pockets, whilst the carboxyl moiety is liganded by hydrogen bonds or salt bridges to basic or polar residues [3,11].

In addition to its function of binding fatty acids tightly, HSA interacts with lipids in another, rather different way, viz., absorbing efficiently to phospholipid membranes [15–18]. Both types of interaction are likely to be involved in the loading and delivery of fatty acids by this transport protein, and hence to contribute to overall control of fatty acid homeostasis. It is

* Corresponding author.
E-mail address: bartucci@fis.unical.it (R. Bartucci).

0005-2736/$ - see front matter © 2007 Elsevier B.V. All rights reserved.
doi:10.1016/j.bbamem.2007.02.019

therefore of biophysical relevance to study molecular and dynamic properties both of fatty acids in the association sites of HSA and of HSA/lipid membrane complexes.

Because of their optimum timescale, methods of linear and non-linear continuous-wave electron paramagnetic resonance (EPR) spectroscopy have been used to study the binding of spin-labelled stearic acids to serum albumin [5,9,12,19,20], and the interaction of HSA with lipid membranes [17,21]. However, more direct and detailed insight into the structure and dynamics of spin-labelled biosystems can be gained by using spin echo-methods of pulsed EPR, both echo-detected (ED) EPR spectra [22–24] and electron spin echo envelope modulation (ESEEM) spectroscopy [25–27]. As applied to spin labels, these methods have, so far, not been used for characterisation of ligand binding sites in proteins, or of the interaction of lipids with membrane proteins. ED-EPR experiments have provided details of the torsional librations at low temperature for small spin labels dissolved in glass-forming media [23,24], and more recently for phospholipid model membranes as a function of chain segment position [28–31]. Such librational motions are present also at higher temperatures, and can form the basis for fluctuations that drive functionally important dynamic changes in the physiological range. Until now, ED-spectra have been used to characterise lipid librational dynamics only in a bilayer environment; therefore, the extension to lipid chains bound to proteins would represent a significant advance in the application of this pulsed EPR methodology to biological membranes. ^{2}H-ESEEM experiments have been performed to detect penetration of water (D_2O) directly in different regions of spin-labelled detergent micelles [32]. The method has been further applied to obtain structural information about ordering, chain packing and degree of hydration in frozen anionic and cationic vesicles [33,34], and to delineate the conformation of the spin probe, and the location of the nitroxide moiety relative to the vesicle–water interface and surfactant headgroups [35]. Recently, ^{2}H-ESEEM spectroscopy has also been used to map out the transmembrane polarity profile in lipid bilayers [31,36–38] and to locate the position of specific regions of membrane-active peptides within model membranes [39,40].

In the present work, we have spin labelled HSA with stearic acids having the nitroxide moiety at different selected positions, *n*, along the alkyl chain (*n*-SASL). We use ED-EPR spectra and D_2O-ESEEM spectra of *n*-SASL to investigate the librational motion of stearic acid in the binding site of human serum albumin, and the accessibility of the binding site to solvent (D_2O), respectively, throughout the whole length of the bound fatty acid chain. Additionally, we have investigated the effect of protein adsorption on lipid chain librations and water penetration in dipalmitoyl phosphatidylcholine (DPPC) bilayer membranes by using phosphatidylcholine spin-labelled along the *sn*-2 chain, *n*-PCSL. Even at low temperatures, the chain librational dynamics and accessibility to water are found to be very different in the hydrophobic binding site of human serum albumin from those in cholesterol-containing lipid membranes [30,38], but similar to those of a spin label covalently anchored at the protein surface.

2. Materials and methods

2.1. Materials

Essential fatty acid-free and globulin-free human serum albumin (HSA, purity approximately 99%), 1,2-dipalmitoyl-*sn*-glycero-3-phosphocholine (DPPC) and spin-labelled maleimide (5-MSL; 3-maleimido-1-oxyl-2,2,5,5-tetramethylpyrrolidine) were obtained from Sigma/Aldrich (St. Louis, MO). Spin-labelled stearic acids (*n*-SASL; *n*-(4,4-dimethyloxazolidine-*N*-oxyl)stearic acid) were synthesized according to ref. [41]. Phosphatidylcholines spin-labelled in the *sn*-2 chain (*n*-PCSL; 1-acyl-2-[*n*-(4,4-dimethyloxazolidine-*N*-oxyl)stearoyl]-*sn*-glycero-3-phosphocholine) were synthesized by acylating egg lysophosphatidylcholine (from Avanti Polar Lipids, Birmingham, AL) with the corresponding *n*-SASL, according to ref. [42]. Certain spin-label positional isomers (*n*-PCSL, n=5,7,10,12,16) were also obtained from Avanti Polar Lipids. Deuterium Oxide (99.9 atom% ^{2}H) was used as obtained from Sigma.

2.2. Sample preparation

DPPC and 1 mol% of *n*-PCSL were codissolved in chloroform. The solvent was evaporated in a nitrogen gas stream, and then residual traces of solvent were removed by drying under vacuum overnight. The lipids, at a concentration of ca. 100 mg/ml, were dispersed with a solution of HSA in D_2O (protein/lipid ratio 1:1 w/w) by vortex mixing whilst heating to above the chain-melting transition of DPPC. The hydrated samples were transferred to a standard 4-mm diameter, quartz EPR tube, concentrated by pelletting in a bench-top centrifuge, and the excess water was removed. Samples were incubated for 24 h at 10 °C before measuring. Aqueous HSA was spin-labelled with stearic acid, *n*-SASL, at equimolar ratios from a dry film. The required amount of *n*-SASL in ethanol stock solution was dried down in a glass vial by using a stream of nitrogen gas, and traces of residual solvent were removed under vacuum. A solution of HSA in D_2O was added and the spin label was taken up by incubation at 45 °C for 30 min with periodic vortex mixing. The spin-labelled protein solution was then transferred to a quartz EPR tube. The final concentration of both HSA and *n*-SASL was 1 mM. Alternatively, HSA was spin-labelled covalently on the single free cysteine residue (Cys34) by reaction with the nitroxide derivative of maleimide, 5-MSL. Maleimide spin label dried down from ethanol was mixed with HSA in buffer at a fivefold molar excess. The mixture was incubated for 24 h at 4 °C with periodic gentle vortexing. Excess free spin label was then separated from the spin-labelled protein by extensive dialysis at 4 °C. After covalently labelling, the sample was handled in the same manner as for HSA with spin-labelled fatty acid bound.

2.3. EPR spectroscopy

Pulsed EPR data were collected on an ELEXSYS E580 9-GHz Fourier Transform FT-EPR spectrometer (Bruker, Germany) equipped with a MD5 dielectric resonator and a CF 935P cryostat (Oxford Instruments, UK). Two-pulse (π/2-τ-π-τ-echo) echo-detected EPR spectra were obtained by recording the integrated spin-echo signal whilst sweeping the magnetic field. The integration window was 160 ns. The microwave pulse widths were 32 ns and 64 ns, with the microwave power adjusted to provide π/2 and π-pulses, respectively.

The original ED-spectra, $ED_T(2\tau,B)$, were corrected for instantaneous spin diffusion by normalising with respect to those recorded at 77 K, where no molecular motion is expected. The corrected spectra, $ED_T^{corr}(2\tau,B)$, recorded at temperature T are plotted as a function of magnetic field, B, according to ref. [29]:

$$ED_T^{corr}(2\tau,B) = ED_T(2\tau,B)\frac{ED_{77K}(2\tau_0,B)}{ED_{77K}(2\tau,B)} \quad (1)$$

where τ_0 is the shortest value of τ for which ED-spectra were recorded. Relaxation rates, $W(B,\tau_1,\tau_2)$, were determined from the ratio of ED-spectra recorded at two different values, τ_1 and τ_2, of the interpulse delay by using the following relation [30]:

$$W(B,\tau_1,\tau_2) = \ln\left[\frac{ED(2\tau_1,B)}{ED(2\tau_2,B)}\right]\cdot\frac{1}{2(\tau_2-\tau_1)} \quad (2)$$

where ED(2τ,*B*) is the ED-spectral lineheight at field position *B*. These relaxation rates are averaged over the time interval from τ_1 to τ_2, and are characterised by the maximum values, W_L and W_H, determined in the low- and high-field regions, respectively, of the ED-spectra. Calibration of the W_L and W_H relaxation rates in terms of the amplitude-correlation time product, $<\alpha^2>\tau_c$, for rotational motion arising from low-amplitude angular librations is taken from the results of spectral simulations reported in ref. [30]. Here, α is the angular amplitude, τ_c is the correlation time, and angular brackets indicate an average over the librational motion.

To obtain ESEEM spectra, three-pulse, stimulated echo (π/2-τ-π/2-*T*-π/2-τ-echo) decays were collected by using microwave pulse widths of 12 ns, with the microwave power adjusted to give π/2-pulses. The time delay *T* between the second and the third pulses was incremented from 20 ns by 700 steps of 12 ns, whilst maintaining the separation τ between the first and the second pulses constant at 168 ns. A four-step phase-cycling program was used to eliminate unwanted echoes. The data were processed to yield standardized ESEEM intensities, as follows: (1) the average experimental echo decay was fitted with a biexponential function; (2) the data were then divided by the fitted average decay function, so that only oscillations about unity remained; (3) the unit level was subtracted from the signal; (4) three levels of zero filling were added at the end of the ESEEM data to increase the total number of points to 4K; and (5) numerical Fourier transformation was performed to obtain an absolute-value ESEEM spectrum. Further details are given in ref. [38].

Conventional, continuous-wave (CW) EPR spectra were acquired on an ESP-300 9-GHz spectrometer equipped with a ER 4201 rectangular TE_{102} ESR cavity and a ER 4111VT temperature controller (Bruker, Karlsruhe, Germany). Spectra were recorded at a microwave power well below saturation and with 100-kHz field modulation.

3. Results

3.1. ED-EPR spectra of DPPC membranes

Fig. 1 shows the corrected echo-detected EPR spectra of the 5-PCSL spin label in bilayer membranes of DPPC, in the presence (solid lines) and in the absence (dotted lines) of excess human serum albumin, at 200 K. The dependence of the lineshapes on the echo delay time, τ, is characteristic of librational motion, as is seen from the preferential decay in the intermediate spectral regions at low and high field with increasing τ (see, e.g., refs. [23,24]). Similar ED-EPR spectral lineshapes are obtained from membranes in the presence and in the absence of adsorbed protein. Only small quantitative differences are seen in the decay rates at the intermediate field positions.

Table 1 gives the maximum values, W_L and W_H, of the ED-EPR relaxation rates deduced from low- and high-field spectral regions, respectively, for both the 5-PCSL and 14-PCSL spin labels in membranes of DPPC, in the presence and in the absence of excess HSA. Essentially consistent rates are obtained between the low- and high-field regions of the ED-spectrum after correction for the different intrinsic sensitivities of W_L and W_H to librational motion (see ref. [30]). The relaxation rates are quite low at 150 K, but become appreciable at 200 K. At 200 K, the relaxation rates are very similar for both label positions. The absolute values of W_L and W_H for samples containing excess HSA are rather similar to those obtained in the absence of protein, for both 5-PCSL and 14-PCSL, and especially for the latter.

3.2. ED-spectra of fatty acid bound to serum albumin

Fig. 2 shows the corrected ED-EPR spectra of the 5-SASL bound to human serum albumin, at 200 K. The dependence of the lineshapes on the echo delay time is qualitatively similar to that for the spin-labelled lipid chains in bilayer membranes (cf. Fig. 1), and again is characteristic of low-amplitude librational motion. Fig. 3a shows the temperature dependence of the maximum values, W_L and W_H, of the ED-EPR relaxation rates, for the 5- and 16-SASL spin labels bound to human serum albumin. The temperature profiles of W_L (solid symbols) and W_H (open symbols) are very similar, showing consistency between the low- and high-field regions of the ED-spectrum. The different absolute values of W_L and W_H arise simply because of the different inherent sensitivities of the low and high-field regions to librational motion [30]. It is seen from Fig. 3a that the intensity of librational motion (i.e., the value of the amplitude-correlation time product $<\alpha^2>\tau_c$) is the same for 16-SASL (squares), at the end of the chain, as it is for 5-SASL (circles) where the spin label is closer to the fatty acid carboxyl group, throughout the entire temperature range. The librational motion of the fatty acid bound to serum albumin is suppressed up to temperatures of ca. 150–160 K. In this low-temperature range, any residual motion is no greater than at 77 K. This is a feature that is shared with spin-labelled chains in DPPC alone (see Table 1 at 150 K), but not in DPPC with equimolar cholesterol (see ref. [30]). Also, the relaxation rates at 200 K of 5-SASL and 16-SASL bound to HSA are comparable to those

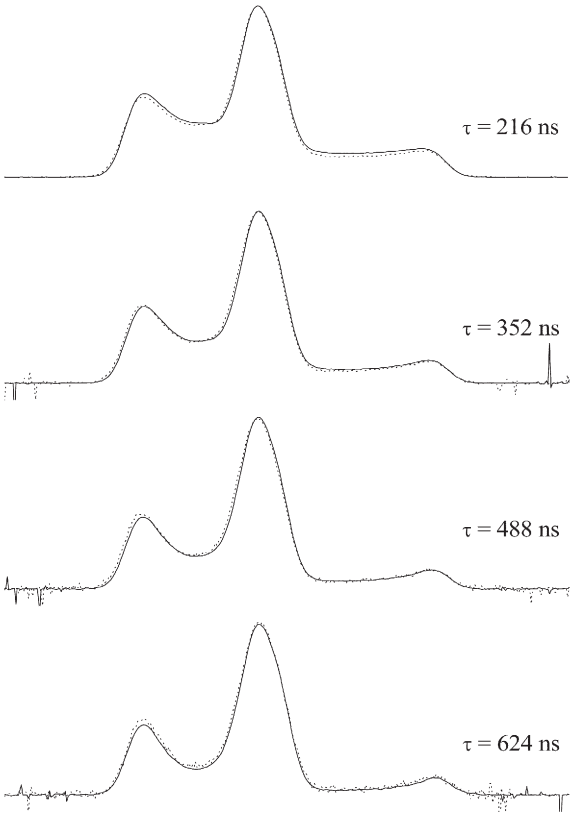

Fig. 1. Echo-detected EPR spectra of the spin-labelled phospholipid 5-PCSL in bilayer membranes of DPPC, in the presence (solid lines) and absence (dotted lines) of excess human serum albumin at 200 K. ED-spectra are recorded for interpulse spacings of (top to bottom) τ=216, 352, 488 and 624 ns, as indicated. Spectra are corrected for instantaneous spin diffusion according to Eq. (1), and are normalised to the maximum lineheight. Total scan width=120 gauss.

Table 1
ED-EPR relaxation-rate parameters, W_L and W_H, for *n*-PCSL spin labels in DPPC bilayer membranes, in the presence and absence of excess human serum albumin[a]

Sample	Spin-label	T (K)	W_L (MHz)	W_H (MHz)
DPPC	5-PCSL	150	0.05±0.02	0.17±0.03
DPPC+HSA	5-PCSL	150	0.11±0.02	0.24±0.02
DPPC	14-PCSL	150	0.25±0.02	0.59±0.06
DPPC+HSA	14-PCSL	150	0.27±0.02	0.59±0.04
DPPC	5-PCSL	200	0.8±0.1	1.73±0.23
DPPC+HSA	5-PCSL	200	0.96±0.03	2.02±0.07
DPPC	14-PCSL	200	0.76±0.01	1.79±0.08
DPPC+HSA	14-PCSL	200	0.79±0.02	1.77±0.07

[a] Determinations of W are for pairs of ED-EPR spectra with τ_1=216 ns and τ_2=352, τ_1=216 ns and τ_2=488 ns, τ_1=216 ns and τ_2=624 ns (see Eq. (2)).

of 5-PCSL and 14-PCSL in DPPC at the same temperature (compare Table 1 and Fig. 3a). Essentially similar results were obtained on lowering the fatty acid spin label/HSA ratio by a factor of 2 or 4.

HSA was spin-labelled with 5-MSL on residue Cys34, which is situated in the loop connecting helices 2 and 3 in the N-terminal region [11]. The temperature dependence of the W-relaxation parameters that is deduced from the ED-spectra (data not shown) is very similar to that of the stearic acid spin labels in the HSA binding site (cf. Fig. 3a), even at the highest temperatures, for which ED-spectra could be recorded.

Fig. 3b shows the dependence of the outer hyperfine splitting, $2A'_{zz}$, in the conventional CW EPR spectra on temperature, for 5- and 16-SASL bound to human serum albumin. For small-amplitude fast librations, the mean-square amplitude, $\langle\alpha^2\rangle$, is related to the partially averaged hyperfine splitting, A'_{zz}, by [43]:

$$A'_{zz} = A_{zz} - (A_{zz} - A_{xx})\langle\alpha^2\rangle \quad (3)$$

where the prime indicates the motionally averaged hyperfine tensor of principal elements A_{xx}, A_{yy} and A_{zz}. The values of A'_{zz} for both 16-SASL (squares) and 5-SASL (circles) remain rather

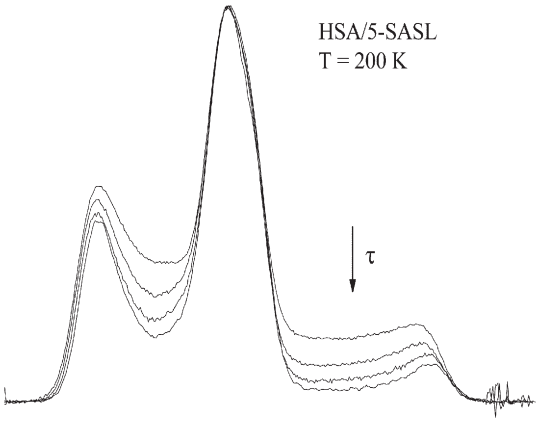

Fig. 2. Echo-detected EPR spectra of the spin-labelled fatty acid 5-SASL bound to aqueous human serum albumin, at 200 K. ED-spectra are recorded for interpulse spacings (top to bottom) of τ=168, 296, 424 and 552 ns. Spectra are corrected for instantaneous diffusion according to Eq. (1), and are normalised to the maximum lineheight. Total scan width=100 gauss.

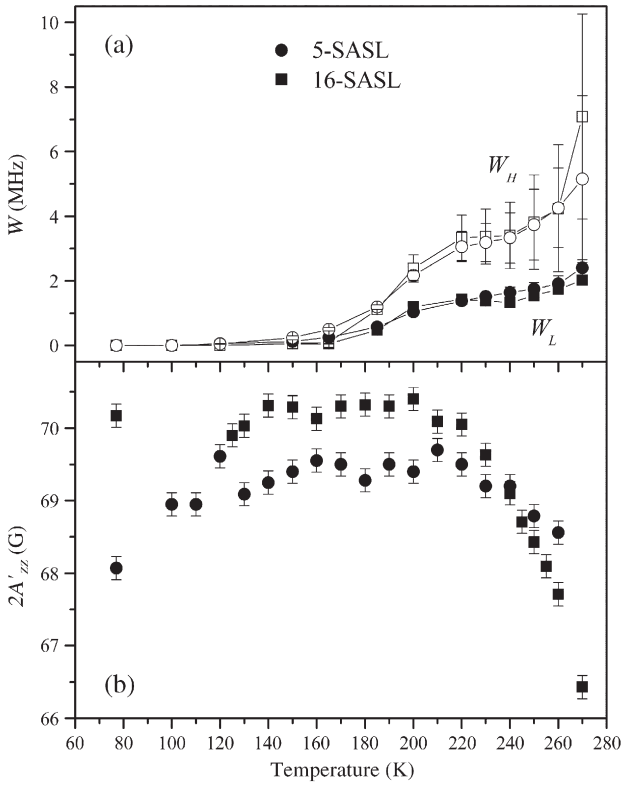

Fig. 3. (a) Temperature dependence of the W_L (solid symbols) and W_H (open symbols) ED-EPR relaxation-rate parameters, for 5-SASL (circles) and 16-SASL (squares) bound to aqueous human serum albumin. Determinations of W are for pairs of ED-EPR spectra with τ_1=168 ns and τ_2=296 ns, τ_1=168 ns and τ_2=424 ns, τ_1=168 ns and τ_2=552 ns (see Eq. (2)). (b) Temperature dependence of the outer hyperfine splitting, $2A'_{zz}$, in the conventional CW-EPR spectra of 5-SASL (circles) and 16-SASL (squares) bound to human serum albumin.

constant up to ca. 200 K. Beyond this, A'_{zz} decreases progressively with increasing temperature for 16-SASL, corresponding to an increasing amplitude of libration. The temperature dependence of the apparent hyperfine splitting for 5-SASL, however, is considerably smaller, possibly because of complicating polarity contributions to A'_{zz} for a label close to the carboxyl group (cf. ref. [30]). (The apparent decrease in A'_{zz} for 5-SASL at 77 K may possibly be an artefactual effect of spin–spin broadening).

Fig. 4a shows the temperature dependence of the librational amplitude-correlation time product, $\langle\alpha^2\rangle\tau_c$, for the 16-SASL fatty acid spin label bound to human serum albumin. These values are obtained from the measurements of W_L given in Fig. 3a, together with the calibration given in ref. [30]. Fig. 4b shows the temperature dependence of the mean-square amplitude, $\langle\alpha^2\rangle$, of the librational motion for the 16-SASL bound to HSA. These values are derived from the motionally averaged hyperfine splittings, according to Eq. (3). The librational amplitude is almost vanishingly small up to 200 K and then increases with increasing temperature. This is consistent with the extremely low relaxation rate and $\langle\alpha^2\rangle\tau_c$ product in the temperature range below 160 K (cf. Figs. 3a and 4a). The largest value of $\langle\alpha^2\rangle$ (at 270 K) corresponds to a root-mean-square amplitude of 14±1°, which confirms that the small-amplitude

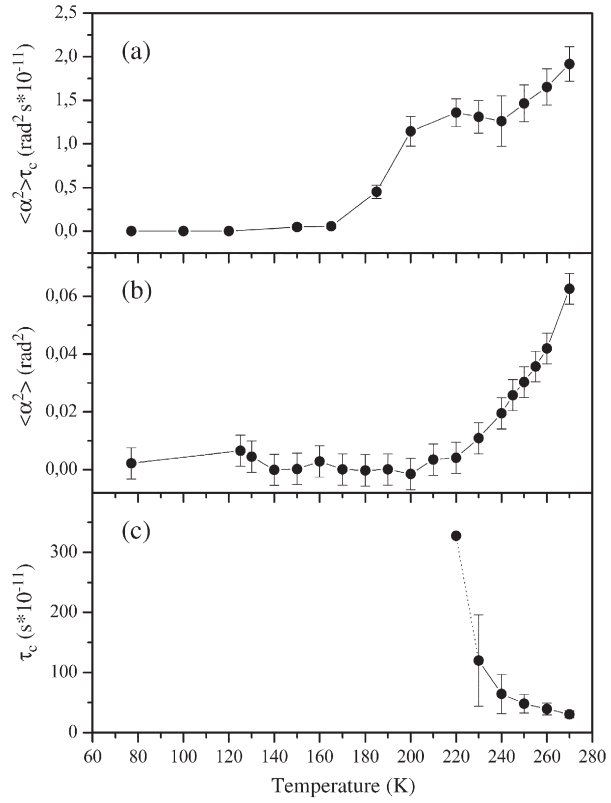

Fig. 4. (a) Temperature dependence of the amplitude-correlation time product, $<\alpha^2>\tau_c$, for 16-SASL bound to human serum albumin. Values are obtained from measurements of the W_L relaxation-rate parameter, together with the results of spectral simulations [30]. (b) Temperature dependence of the librational amplitude, $<\alpha^2>$, for 16-SASL bound to human serum albumin. Values are obtained from the motionally averaged hyperfine splitting, $2A'_{zz}$, together with Eq. (3). (c) Temperature dependence of the librational correlation time, τ_c, for 16-SASL bound to human serum albumin. Values are obtained from the amplitude-correlation product in part (a) and the librational amplitude in part (b).

approximation is appropriate at low temperatures. Fig. 4c shows correspondingly the temperature dependence of the rotational correlation time, τ_c, for the librational motion of 16-SASL bound to human serum albumin. Determinations of the amplitude-correlation time product, $<\alpha^2>\tau_c$, from Fig. 4a were combined with the amplitude (i.e., $<\alpha^2>$) measurements that are given in Fig. 4b to obtain these values for τ_c by simple division. Reliable values are obtained for τ_c only in the region above 200 K, where the amplitude $<\alpha^2>$ becomes appreciably greater than zero. Correlation times at 240 K and above are in the subnanosecond region, which confirms that the librations are in the fast motional regime. The correlation time for 16-SASL decreases quite steeply with increasing temperature in this range. The librational motion of the bound fatty acid apparently is an activated process. The low amplitudes at temperatures lower than 240 K, however, prevent firm conclusions to be reached about the temperature dependence in the lower range.

From the similarity in relaxation rates and amplitude-correlation time products for the two spin-label positions (Figs. 3a and 4a), it may be surmised that the correlation times for 5-SASL are similar to those for 16-SASL at 240 K and above. However, from Fig. 3b, it cannot be excluded that τ_c for 5-SASL is somewhat longer than that for 16-SASL at temperatures above 240 K.

3.3. ESEEM spectra of DPPC membranes

Fig. 5 shows absolute-value ESEEM spectra for spin-labelled phosphatidylcholine, *n*-PCSL, in DPPC bilayers, in the presence and absence of human serum albumin. The inter-pulse separation, τ, between the first and second pulses was set equal to 168 ns to maximize the deuterium and proton modulations simultaneously, in each case. Lines are seen in the ESEEM spectra of 5-PCSL that are centred around the deuterium Larmor frequency at ca. 2.6 MHz and around that of protons at 14.6 MHz. The latter originates primarily from matrix protons. The ^{2}H-ESEEM spectra consist of a sharp and a broad component that arise from free intramembranous D_2O and from D_2O that is hydrogen bonded to the spin-label nitroxide group, respectively [38]. The total intensity of the 5-PCSL D_2O-ESEEM spectrum is similar for bilayers of DPPC in the presence and absence of human serum albumin. For 14-PCSL, the nitroxide of which is situated deeper in the bilayer, the deuterium ESEEM spectrum is almost completely absent, both in the presence and in the absence of HSA.

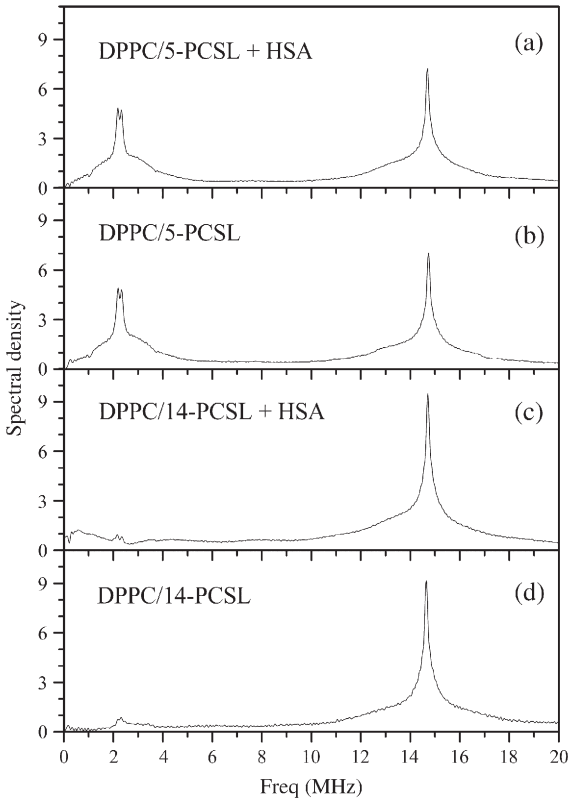

Fig. 5. Fourier-transform ESEEM spectra at 77 K for spin-labelled phosphatidylcholines (*n*-PCSL) in DPPC membranes in the presence and absence of excess human serum albumin and hydrated in D_2O. (a) 5-PCSL in DPPC, in the presence of human serum albumin. (b) 5-PCSL in DPPC alone. (c) 14-PCSL in DPPC, in the presence of human serum albumin. (d) 14-PCSL in DPPC alone.

Fig. 6 shows the dependence on spin-label position, n, of the maximum amplitudes of the deuterium ESEEM spectra for DPPC bilayers in the absence of human serum albumin (open circles). The amplitude of the lines was measured as the total spectral density at 2.2 MHz, i.e., the broad plus sharp components, whose ratio remains constant, independent of spin-label position [38]. For DPPC alone, the amplitudes of the D_2O ESEEM spectra display a sharp change in amplitude at an intermediate chain position, the location of which is somewhat imprecisely defined because of the effects of spin–spin broadening [38]. Measurements with n-PCSL display a similar trend in the presence of human serum albumin (solid squares in Fig. 6). The ^{2}H-modulation amplitude decreases on proceeding deeper into the membrane, corresponding to decreasing local concentration of intramembranous water (D_2O) [38]. The profile of water penetration into the membrane is therefore disturbed very little, if at all, by the adsorption of human serum albumin at the membrane surface.

3.4. ESEEM spectra of fatty acid bound to serum albumin

Fig. 7 shows absolute-value ESEEM spectra for n-SASL bound to human serum albumin in D_2O solution. ESEEM spectra from samples with 2 or 4 times lower 5-SASL/HSA ratios do not differ significantly from that shown in Fig. 7. For all spin-labelled chain segments, $n=5$ to 16, the ESEEM spectra contain peaks at the deuterium NMR frequency, in addition to those at the proton frequency. The ^{2}H-ESEEM spectra again consist of a broad and a sharp component that arise from D_2O that either is hydrogen bonded to the spin-label nitroxide group or is not hydrogen bonded, respectively. (The broad component is therefore determined by the local accessibility of water to the spin label, and not by water bound at remote locations). Intensities of the ^{2}H-ESEEM spectra from n-SASL bound to human serum albumin are much greater than those from n-PCSL in DPPC bilayers, even for the $n=5$ position which is closest to the lipid polar headgroup. The dependence of the overall ^{2}H-ESEEM intensity (i.e., the sum of the sharp and broad components) on chain segment position of the bound fatty acid is included in Fig. 6, and contrasts sharply with that for the spin-labelled lipid chains in bilayer membranes. The ^{2}H-ESEEM intensity is much more uniform along the bound fatty acid chain than in lipid bilayers, with a shallow minimum at around $n=7$ and the highest value for the $n=16$ position, instead of at $n=5$ as in bilayers. The D_2O-ESEEM results for n-SASL bound to HSA are also consistent with the relative outer hyperfine splittings, under conditions where the librational amplitudes are essentially zero (see Fig. 3b). The plateau values of A'_{zz} for 16-SASL are greater than for 5-SASL, corresponding to a higher environmental polarity. The D_2O-ESEEM spectrum of HSA covalently labelled with 5-MSL (data not shown) is qualitatively similar to that of 16-SASL bound to HSA, but is of greater amplitude (see Fig. 6).

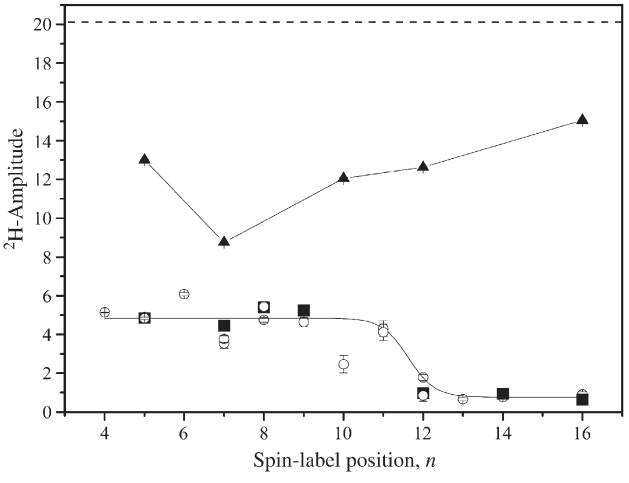

Fig. 6. Dependence on spin-label position, n, of the ^{2}H-ESEEM spectral amplitudes for n-PCSL in DPPC bilayers, in the presence (solid squares) and absence (open circles) of human serum albumin at 77 K. Corresponding data for n-SASL bound to human serum albumin are given by solid triangles. The dashed horizontal line represents the D_2O-ESEEM amplitude of the 5-MSL maleimide spin label that is covalently bound to HSA.

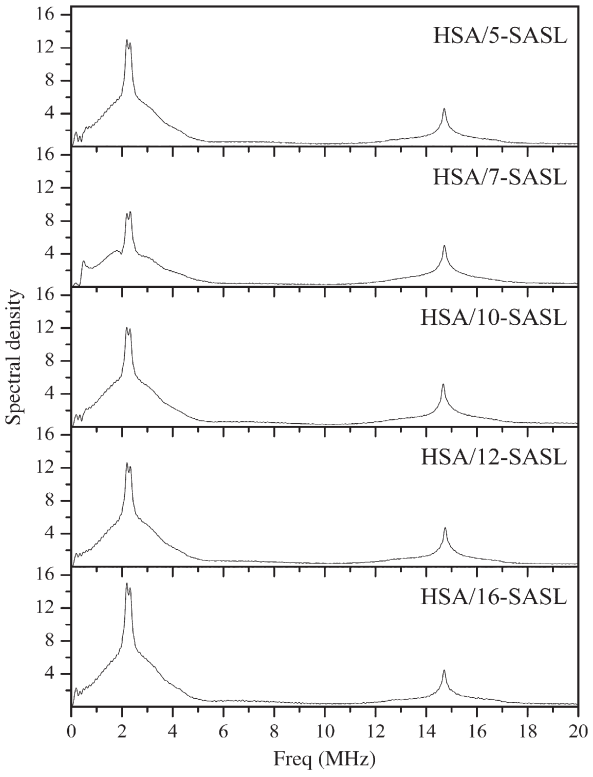

Fig. 7. Fourier-transform ESEEM spectra for spin-labelled stearic acid (n-SASL) bound to human serum albumin in D_2O solution at 77 K. The position of chain spin labelling ($n=5$–16) is indicated on the figure.

4. Discussion

Adsorption of human serum albumin at the surface of DPPC membranes has only small effects on the lipid chain librations at low temperature (see Fig. 1 and Table 1), although it has a pronounced effect on the chain motions in gel and fluid membranes [17]. The effects of protein adsorption are seen, however, on the instantaneous diffusion that arises from spin–spin interactions (see ref. [29]). This is clear in the original ED-

spectra of *n*-PCSL, before correction according to Eq. (1) (data not shown). Surface adsorption of HSA therefore affects the lipid packing density in such a way as to increase spin–spin interactions between the spin-labelled lipid chains. Nevertheless, these changes that are induced by surface association of the protein do not greatly affect the profile of water penetration into the membrane (see Figs. 5 and 6).

Fig. 8 shows the crystal structure of HSA with bound stearic acid [11]. A large excess of fatty acid was used to achieve this high level of occupation in co-crystallisation. Cistola et al. [7,8] have shown that the high-affinity binding sites are those that involve both hydrophobic interactions with the fatty-acid chain and polar interactions with the anionic carboxyl group. This is a feature that is common to sites 1–5 shown in Fig. 8, which are located in domains I and III of the crystal structure. Recently, by using nuclear magnetic resonance drug-competition experiments, it was found that sites 2, 4 and 5 bind long-chain fatty acids (palmitates and stearates) with high affinity [44]. On the basis of biochemical evidence, it is suggested that site 5 in subdomain IIIB may be the site of highest affinity for long-chain fatty acids [10]. This is therefore the site that is likely to be probed here by spin-labelled stearic acid at equimolar ratio with respect to HSA. It should be noted, however, that conventional binding titrations do not resolve a single high-affinity site, which suggests that a second site might be partially populated [45].

The present pulsed EPR experiments reveal major differences between the fatty-acid chain environments in the protein binding site and in the tightly packed low-temperature phases of lipid membranes (cf. refs. [30,38]). The chain dynamics at low temperature (< 200 K) are considerably more restricted in the protein binding site than in frozen bilayer membranes of DPPC containing equimolar cholesterol (compare Fig. 3 with Fig. 4 of ref. [30]. The latter have a cholesterol content similar to that of the plasma membranes with which serum is in contact. Further, there is no preferential enhancement of mobility towards the terminal methyl end of the fatty-acid chain in the HSA binding site (i.e., of 16-SASL relative to 5-SASL) such as is seen for 14-PCSL relative to 5-PCSL in DPPC membranes with 50 mol% cholesterol (see ref. [30]). The methyl terminus of the fatty-acid chain is as strongly restricted in the hydrophobic binding site as is the carboxyl headgroup at the ionic association site, in HSA. CW-ESR measurements at 293 K on albumin/*n*-SASL also reveal that the rotational dynamics of the stearates are hindered in the protein pocket, although the terminal methyl end shows greater motion (5, 9, 12, 21). These dynamic results on the fatty-acid binding are essentially consistent with the structure of site 5 in HSA crystals (see Fig. 8). In site 5, the carboxylate interacts with the positively charged side-chain of Lys525 and also with Tyr401; and the fatty-acid chain is confined in a hydrophobic channel that spans the width of sub-domain IIIB [11].

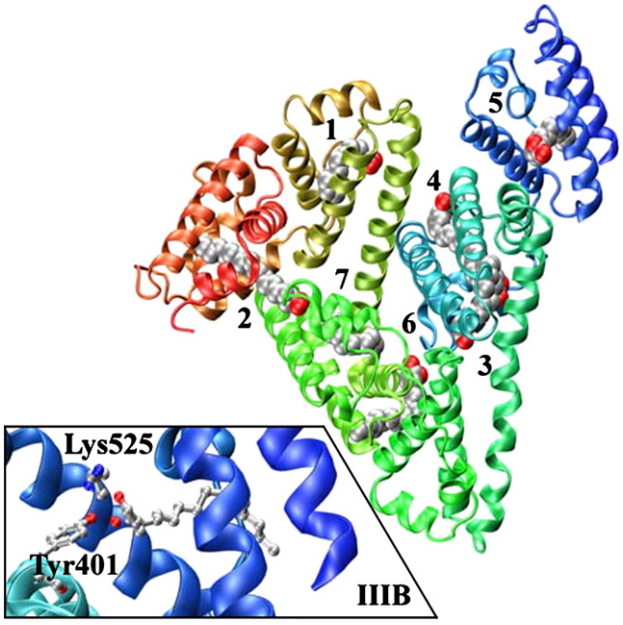

Fig. 8. Crystal structure of HSA [11; PDB code: 1E7I] indicating the location of the binding sites for stearic acid (1–7). Inset: stearic acid bound to site 5 in subdomain IIIB.

The D_2O-ESEEM experiments reveal other features relevant to the architecture of the hydrophobic binding pocket in human serum albumin. Chain segments adjacent to the polar carboxyl group are not the only ones that are readily accessible to water in the fatty acid binding site. Water accessibility is preserved throughout the whole length of the bound fatty acid chain (see Fig. 6). Unlike the lipid chains in bilayer membranes, the terminal methyl group is equally accessible to water as the carboxyl region of the chain. This feature of the binding site evidenced by ESEEM results could facilitate exchange of lipids via the aqueous phase. Exchange of fatty acids takes place readily between human serum albumin and donor/acceptor membranes in the fluid state (see, e.g., refs. [21,46]). The spin-label results on water accessibility are consistent with the structure of binding site 5 (see Fig. 8) insofar as the terminal methyl group of stearic acid projects through the far side of the hydrophobic channel and so is exposed to solvent rather than being buried within the hydrophobic interior [11]. More indirect experiments with aqueous paramagnetic relaxation agents reveal a pattern of accessibility to spin-labelled fatty acids in the binding sites of serum albumin which is similar to that found here directly for D_2O accessibilities [12]. The relaxation enhancement of 16-SASL by ferricyanide in solution was found to be greater than that of 5-SASL or 12-SASL, in agreement with the relative ^{2}H-ESEEM intensities.

The absolute values of the D_2O-ESEEM modulation intensities are also significant. They are much greater in the binding site of HSA than in DPPC alone, at all positions of chain-labelling. The values for *n*-SASL bound to HSA are comparable to, or greater than, those obtained for label positions close to the lipid polar headgroups (n=4–6) in bilayers of DPPC plus 50 mol% cholesterol and are far greater than those close to the methyl terminal (n=10–14) of the chains in the same membranes (cf. ref. [38]). Density functional (DFT) calculations predict that the normalised ^{2}H-ESEEM intensity for one D_2O molecule hydrogen-bonded to the nitroxide is $I_o \approx 9.5$ [38]. Thus, from the intensities of the broad D_2O-ESEEM components in Fig. 7, it can be estimated that the fraction of fatty-acid nitroxides that are hydrogen bonded to

water varies from maximally $I/I_o = 0.44 \pm 0.05$ to 0.70 ± 0.05 for $n = 7$ and 16, respectively, in the binding site of HSA. It was shown further in ref. [38], by application of the mass-action law, that the product of the equilibrium constant, K, for hydrogen bonding and the effective concentration of free water, $[W]$, is given by:

$$K[W] = \frac{I/I_o}{2 - I/I_o} \quad (4)$$

where I is the normalised intensity of the broad D_2O-ESEEM component. Hence, these values vary from $K[W] = 0.28 \pm 0.04$ to 0.54 ± 0.06 for 7-SASL and 16-SASL, respectively, when bound to HSA. Correspondingly, the fraction of nitroxides that are H-bonded by a single water molecule varies from 0.34 ± 0.03 to 0.46 ± 0.02, and of those that are H-bonded by two water molecules varies from 0.05 ± 0.01 to 0.12 ± 0.02, for 7-SASL and 16-SASL bound to HSA, respectively. For comparison, the maximum values that are obtained in lipid bilayers (at position $n = 4$) are: $K[W] = 0.12$ and 0.31, with fractions H-bonding to one water of 0.20 and 0.36, and fractions H-bonding to two waters of 0.01 and 0.06, for DPPC and DPPC +50 mol% cholesterol, respectively [38]. These results again emphasize the difference in accessibility to water of the fatty-acid binding site in HSA from that in the interior of lipid membranes.

It is of considerable interest also to compare the spin-echo data obtained on spin-labelled fatty acids in the binding site of HSA with those from 5-MSL, a site-specific spin label that is covalently attached at the protein surface. It appears that the small-amplitude librational motions of the bound fatty acids are rather similar to those of a spin label that is covalently anchored to the backbone of a surface-exposed loop. The water exposure of fatty acids in the HSA binding site, although somewhat smaller, is comparable to that of a surface residue in the protein. Such a situation should facilitate exchange of fatty acids whilst still providing tight binding.

Acknowledgements

We thank Frau B. Angerstein for synthesis of spin-labelled phospholipids. The two groups are members of the COST P15 Action of the European Union.

References

[1] T. Peters, All About Albumin: Biochemistry, Genetics and Medical Applications, Academic Press, San Diego, 1995.
[2] J.R. Brown, P. Shockley, Serum albumin structure and characterization of its ligand binding sites, in: P.C. Jost, O.H. Griffith (Eds.), Lipid–Protein Interactions, vol. 1, Wiley and Sons, New York, 1982, pp. 26–68.
[3] X.M. He, D.C. Carter, Atomic structure and chemistry of human serum albumin, Nature 358 (1992) 209–215.
[4] A.A. Spector, Fatty acid binding to plasma albumin, J. Lipid Res. 16 (1975) 165–188.
[5] H.H. Ruf, M. Gratzl, Binding of nitroxide stearate spin labels to bovine serum albumin, Biochim. Biophys. Acta 446 (1976) 134–142.
[6] J.A. Hamilton, D.P. Cistola, J.D. Morrisett, J.T. Sparrow, D.M. Small, Interactions of myristic acid with bovine serum albumin: a ^{13}C NMR study, Proc. Natl. Acad. Sci. U. S. A. 81 (1984) 3718–3722.
[7] D.P. Cistola, D.M. Small, J.A. Hamilton, Carbon ^{13}NMR studies of saturated fatty acids bound to bovine serum albumin: I. The filling of individual fatty acid binding sites, J. Biol. Chem. 262 (1987) 10971–10979.
[8] D.P. Cistola, D.M. Small, J.A. Hamilton, Carbon ^{13}NMR studies of saturated fatty acids bound to bovine serum albumin: II. Electrostatic interactions in individual fatty acid binding sites, J. Biol. Chem. 262 (1987) 10980–10985.
[9] M. Ge, S.B. Ranavare, J.H. Freed, ESR studies of stearic acid binding to bovine serum albumin, Biochim. Biophys. Acta 1036 (1990) 228–236.
[10] S. Curry, P. Brick, N.P. Franks, Fatty acid binding to human serum albumin: new insights from crystallographic studies, Biochim. Biophys. Acta 1441 (1999) 131–140.
[11] A.A. Bhattacharya, T. Gruene, S. Curry, Crystallographic analysis reveals common modes of binding of medium and long-chain fatty acids to human serum albumin, J. Mol. Biol. 303 (2000) 721–732.
[12] V.A. Livshits, D. Marsh, Fatty acid binding sites of serum albumin probed by non-linear spin-label EPR, Biochim. Biophys. Acta 1466 (2000) 350–360.
[13] J.-K. Choi, J. Ho, S. Curry, D. Quin, R. Bittman, J.A. Hamilton, Interactions of very long-chain saturated fatty acids with serum albumin, J. Lipid Res. 43 (2002) 1000–1010.
[14] J.R. Simard, P.A. Zunszain, C.-E. Ha, J.S. Yang, N.V. Bhagavan, I. Petitpas, S. Curry, J.A. Hamilton, Locating high-affinity fatty acid-binding sites on albumin by X-ray crystallography and NMR spectroscopy, Proc. Natl. Acad. Sci. U. S. A. 102 (2005) 17958–17963.
[15] M.N. Dimitrova, H. Matsamura, A. Dimitrova, V.Z. Neitchev, Interaction of albumins from different species with phospholipid liposomes. Multiple binding sites system, Inter. J. Biol. Macromol. 27 (2000) 187–194.
[16] R. Galantai, I. Bardos-Nagy, The interaction of human serum albumin and model membranes, Int. J. Pharm. 195 (2000) 207–218.
[17] R. Bartucci, M. Pantusa, D. Marsh, L. Sportelli, Interaction of human serum albumin with membranes containing polymer-grafted lipids: spin-label ESR studies in the mushroom and brush regimes, Biochim. Biophys. Acta 1564 (2002) 237–242.
[18] X. Wang, Q. He, S. Zheng, G. Brezesinski, H. Mohwald, J. Li, Structural changes of phospholipid monolayers caused by coupling of human serum albumin: a GIXD study at the air/water interface, J. Phys. Chem., B 108 (2004) 14171–14177.
[19] J.D. Morrisett, H.J. Pownall, A.M. Gotto Jr., Bovine serum albumin. Study of the fatty acid and steroid binding sites using spin-labelled lipids, J. Biol. Chem. 250 (1975) 2487–2494.
[20] R.C. Perkins Jr., N. Abumrad, K. Balasubramanian, L.R. Dalton, A.H. Beth, J.H. Park, C.R. Park, Equilibrium binding of spin-labeled fatty acids to bovine serum albumin: suitability as surrogate ligands for natural fatty acids, Biochemistry 21 (1982) 4059–4064.
[21] M. Pantusa, L. Sportelli, R. Bartucci, Transfer of stearic acids from albumin to polymer-grafted lipid containing membranes probed by spin-label electron spin resonance, Biophys. Chem. 114 (2005) 121–127.
[22] G.L. Millhauser, J.H. Freed, Two-dimensional electron spin echo spectroscopy and slow motions, J. Chem. Phys. 81 (1984) 37–48.
[23] S.A. Dzuba, Yu. D. Tsvetkov, A.G. Maryasov, Echo-detected EPR spectra of nitroxides in organic glasses: model of orientational molecular motions near equilibrium position, Chem. Phys. Lett. 188 (1992) 217–222.
[24] S.A. Dzuba, Librational motion of guest spin probe molecules in glassy media, Phys. Lett., A 213 (1996) 77–84.
[25] L. Kevan, M.K. Bowman, Modern Pulsed and Continuous-Wave Electron Spin Resonance, Wiley and Sons, New York, 1990.
[26] S.A. Dikanov, Yu. D. Tsvetkov, Electron Spin Echo Envelope Modulation (ESEEM) Spectroscopy, CRC Press, Boca Raton, FL, 1992.
[27] A. Schweiger, G. Jeschke, Principles of Pulse Electron Paramagnetic Resonance, Oxford University Press, New York, 2001.
[28] R. Bartucci, R. Guzzi, D. Marsh, L. Sportelli, Chain dynamics in the low-temperature phases of lipid membranes by electron spin-echo spectroscopy, J. Magn. Reson. 162 (2003) 371–379.
[29] D.A. Erilov, R. Bartucci, R. Guzzi, D. Marsh, S.A. Dzuba, L. Sportelli, Echo-detected electron paramagnetic resonance spectra of spin-labeled lipids in membrane model systems, J. Phys. Chem., B 108 (2004) 4501–4507.

[30] D.A. Erilov, R. Bartucci, R. Guzzi, D. Marsh, S.A. Dzuba, L. Sportelli, Librational motion of spin-labeled lipids in high-cholesterol containing membranes from echo-detected EPR spectra, Biophys. J. 87 (2004) 3873–3881.
[31] R. Bartucci, D.A. Erilov, R. Guzzi, L. Sportelli, S.A. Dzuba, D. Marsh, Time-resolved electron spin resonance studies of spin-labelled lipids in membranes, Chem. Phys. Lipids 141 (2006) 142–157.
[32] E. Szajdzinska-Pietek, R. Maldonado, L. Kevan, R.R.M. Jones, Electron spin resonance and electron spin echo modulation studies of *N,N,N′,N′*-tetramethylbenzidine photoionizaton in anionic micelles: structural effects of tetramethylammonium cation counterion substitution for sodium cation in dodecyl sulphate micelles, J. Am. Chem. Soc. 106 (1984) 4675–4678.
[33] T. Hiff, L. Kevan, Electron spin echo modulation studies of doxylstearic acid spin probes in frozen vesicles: interaction of the spin probe with D_2O and effects of cholesterol addition, J. Phys. Chem. 93 (1989) 1572–1575.
[34] P. Bratt, H.J.D. McManus, L. Kevan, Electron spin echo modulation studies of doxylstearic acid spin probes in frozen dihexadecyl phosphate and dioctadecyldimethylammonium chloride vesicles: interaction of the spin probe with deuterated water and effects of cholesterol addition, J. Phys. Chem. 96 (1992) 5093–5096.
[35] V.V. Kurshev, L. Kevan, Electron spin echo modulation studies of doxylstearic acid spin probes in frozen vesicle solutions: interaction of the spin probe with 31P in the surfactant headgroups, J. Phys. Chem. 99 (1995) 10616–10620.
[36] R. Bartucci, R. Guzzi, D. Marsh, L. Sportelli, Intramembrane polarity by electron spin echo spectroscopy of labeled lipids, Biophys. J. 84 (2003) 1025–1030.
[37] V. Noethig-Laslo, P. Cevc, D. Arcon, M. Sentjurc, Comparison of CW-EPR and ESEEM technique for determination of water permeability profile in liposome membranes, Appl. Magn. Reson. 27 (2004) 303–309.
[38] D.A. Erilov, R. Bartucci, R. Guzzi, A.A. Shubin, A.G. Maryasov, D. Marsh, S.A. Dzuba, L. Sportelli, Water concentration profiles in membranes measured by ESEEM of spin-labeled lipids, J. Phys. Chem., B 109 (2005) 12003–12013.
[39] R. Carmieli, N. Capo, H. Zimmermann, A. Potapov, Y. Shai, D. Goldfarb, Utilising ESEEM spectroscopy to locate the position of specific regions of membrane-active peptides within model membranes, Biophys. J. 90 (2006) 492–505.
[40] E.S. Salnikov, D.A. Erilov, A.D. Milov, Y.D. Tsvetkov, C. Peggion, F. Formaggio, C. Toniolo, G. Raap, S.A. Dzuba, Location and aggregation of the spin-labeled peptide trichogin GA IV in a phospholipid membrane as revealed by pulsed EPR, Biophys. J. 91 (2006) 1532–1540.
[41] W.L. Hubbell, H.M. McConnell, Molecular motion in spin-labelled phospholipids and membranes, J. Am. Chem. Soc. 93 (1971) 314–326.
[42] D. Marsh, A. Watts, Spin-labeling and lipid–protein interactions in membranes, in: P.C. Jost, O.H. Griffith (Eds.), Lipid–Protein Interactions, vol. 2, Wiley-Interscience, New York, 1982, pp. 53–126.
[43] S.P. Van, G.B. Birrell, O.H. Griffith, Rapid anisotropic motion of spin labels. Models for motional averaging of the ESR parameters, J. Magn. Reson. 15 (1974) 444–459.
[44] J.R. Simard, P.A. Zunszain, J.A. Hamilton, S. Curry, Location of high and low affinity fatty acid binding sites on human serum albumin revealed by NMR drug-competition analysis, J. Mol. Biol. 361 (2006) 336–351.
[45] D.J. Ashbrooke, A.A. Spector, E.C. Santos, J.E. Fletcher, Long chain fatty acid binding to human plasma albumin, J. Biol. Chem. 250 (1975) 2333–2338.
[46] M.S.C. Abreu, L.M.B.B. Estronca, M.J. Moreno, W.L.C. Waz, Binding of a fluorescent lipid amphiphile to albumin and its transfer in lipid bilayer membranes, Biophys. J. 84 (2003) 386–399.